# Study of the nuclear mass composition of UHECR with the surface detectors of the Pierre Auger Observatory

**Hernan Wahlberg *, for the Pierre Auger Collaboration†**

* *Physics Department, Universidad Nacional de La Plata C.C. 67-1900 La Plata, Argentina*
† *Pierre Auger Observatory, Av. San Martin Norte 304, (5613) Malargüe, Prov. De Mendoza, Argentina*

***Abstract*. We investigate observables that can be measured with the water-Cherenkov detectors of the Pierre Auger Observatory. In particular we explore the use of the risetime of the signals in the detectors and the azimuthal features of the time distributions. A correlation of these observables with the position of shower maximum ($X_{\max}$), as measured with the fluorescence telescopes, is obtained.**

***Keywords*: mass composition auger**

## I. Introduction

The Surface Detector Array (SD) of the southern site of the Pierre Auger Observatory [1] consists of 1660 detectors equally spaced on a triangular grid (1.5 km) over an area of approximately 3000 km$^2$. Each SD detector is a water-Cherenkov detector, with electronics that digitises the signals at 40 MHz sampling rate. The Fluorescence Detector (FD) consists of 4 sites with 6 telescopes each located at the border of the SD array overlooking it. The SD records the shower front by sampling the secondary particles at ground level with a duty close to 100%. The FD measures the fluorescence light emitted as the shower develops through the atmosphere. As it can only operate on clear, moonless nights, its duty cycle is about 13%. FD events provide a direct measurement of $X_{\max}$ ([2] and [3]) that, at present, is the main parameter used to infer mass composition. The bulk of events collected at the Observatory have information only from the surface array and therefore observables from SD, as the ones presented in this paper, are important for composition analysis of Ultra High Energy Cosmic Rays (UHECR).

## II. The risetime of the signal

The time profile of particles reaching ground is sensitive to cascade development as the higher the production height the narrower is the time pulse [4]. The first portion of the signal is dominated by the muon ($\mu$) component which arrives earlier and over a period of time shorter than the electromagnetic particles ($em$).

The risetime ($t_{1/2}$) defined as the time to go from 10% to 50% of the total integrated signal in each station, was shown to be effective for mass discrimination. This is because it is sensitive to the $\mu$ to $em$ ratio, a parameter that varies with the primary mass composition, and is highly correlated with the shower development and the depth of its maximum [5].

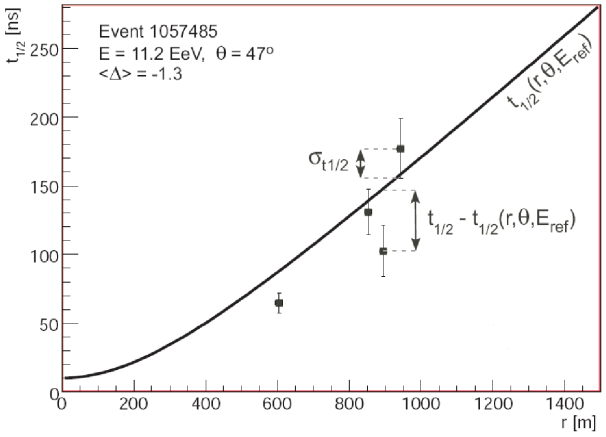


Fig. 1. Risetime vs distance to the core. The curve is the benchmark risetime and the data points represent the measurements of risetime of each detector with uncertainties for this particular event.

A method to obtain the $X_{\max}$ value based on SD observables has been developed. This method consists of obtaining the average value of the risetime as a function of the core distance ($r$) and the zenith angle ($\theta$) for a given reference energy ($10^{19}$ eV), the so-called benchmark. Then, for each selected detector in a given event, the deviation of the measured risetime from the benchmark function is calculated in units of measurement uncertainty and averaged for all detectors in the event as shown in equation 1 and Figure 1, enabling a new observable, $< \Delta_i >$ to be introduced.

$$< \Delta_i >= \frac{1}{N} \sum_{i=1}^{N} \frac{t^i_{1/2} - t_{1/2}(r, \theta, E_{ref})}{\sigma^i_{1/2}(\theta, r, S)}, \qquad (1)$$

where $\sigma^i_{1/2}(\theta, r, S)$ stands for the uncertainty parameterised as function of zenith angle, distance to the core and signal ($S$) of each detector. The $< \Delta_i >$ are expected to be larger for showers developing deeper in the atmosphere than the reference risetime. Figure 2 reflects this fact as the $< \Delta_i >$ is found to increase with energy which is expected as the showers become more penetrating. This parameter has the advantage that can be calculated without any functional adjustment on an event-by-event basis and also it can be determined in events with only one detector satisfying the selection criteria. It is clear from Figure 2 that the rate of change of $< \Delta_i >$ with energy is greater between $3.10^{18}$ and $8.10^{18}$ eV than it is above. Using hybrid events it can be shown that $< \Delta_i >$ is linearly proportional

to $X_{\max}$ (Figure 3), confirming the conclusion reached in [5] from simulations. To improve the accuracy of the correlation, signals for each individual detector are deconvolved using single particle response of the electronics. At present the uncertainties are quite large and calibration of the depth parameter based on risetime is on-going. The results shown at the end in Figure 7 are thus to be regarded as preliminary.

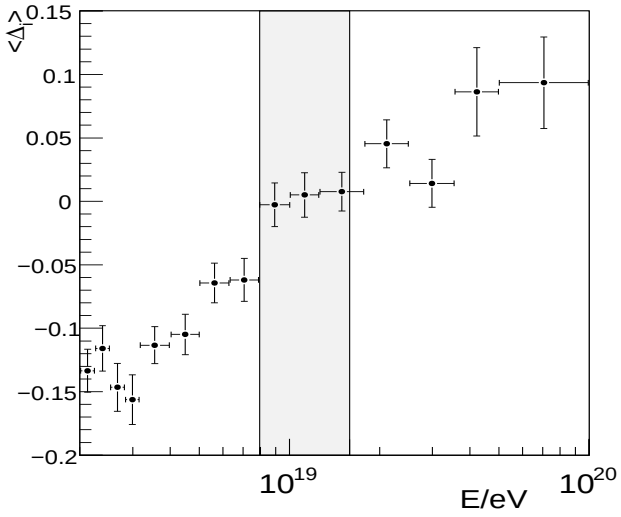


Fig. 2. The average $< \Delta_i >$ as a function of energy for SD events. The dashed lines enclose the region defined for the benchmark function.

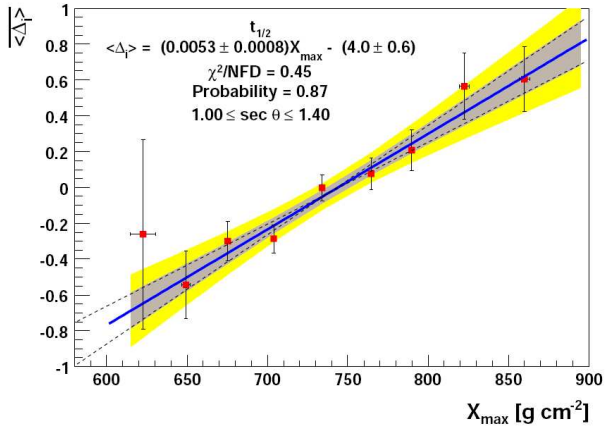


Fig. 3. The average $< \Delta_i >$ as a function of $X_{\max}$ for selected hybrid events. A correlation is found which is parameterised with a linear fit. The shaded areas show the estimated uncertainty (one and two $\sigma$), obtained by fluctuating each point randomly within the measured error bar and repeating the fitting procedure.

## III. Asymmetry in the Shower Development

The azimuthal asymmetry of time distributions from SD detector signals of non-vertical showers carries valuable information related to the chemical composition of cosmic rays ([6] and [7]).

The risetime asymmetry can be measured by selecting events in bins of energy and $\sec\theta$. Then, for these events

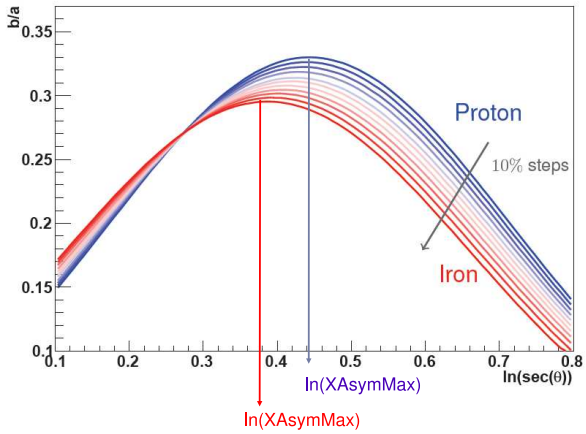


Fig. 4. Asymmetry development for the different samples with mixed composition, going from pure proton to pure iron in steps of 10%. The positions of the maxima for the different primaries are marked.

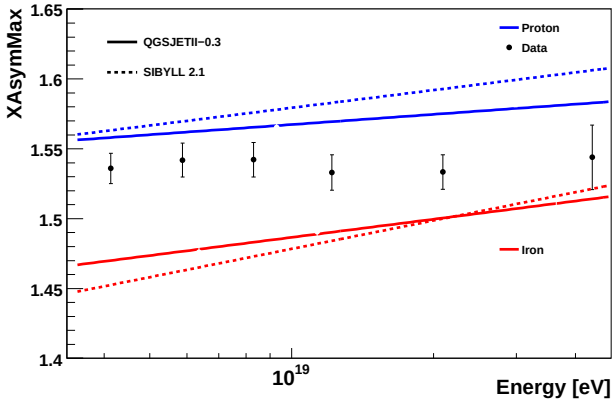


Fig. 5. Position of maximum asymmetry vs. primary energy for different models and primaries. Lines correspond to fitted distributions of MC samples for proton (blue) and iron (red) primaries.

the average risetime[1] of those detectors passing quality cuts is determined. After that, for each ($E$, $\sec\theta$) bin, a fit of $< t_{1/2}/r >$ to a linear cosine function of $\zeta$ (azimuthal angle in the shower plane) provides the asymmetry factor $b/a$ from:

$$< t_{1/2}/r >= a + b\,\cos\zeta \qquad (2)$$

The evolution of $b/a$ with zenith angle is an indicator of the shower development and is different for different primaries as shown in Figure 4. It is worth remarking here, that this method is not based on event-by-event values but is determined by the zenith angle evolution of events grouped in certain energy bins, where a unique value of the asymmetry parameter is obtained for all of them.

In Figure 5 the values of the position ($\sec\theta$) at which the asymmetry longitudinal development reaches its

[1] As the $t_{1/2}$ increases with the core-distance, $t_{1/2}/r$ is more suitable for asymmetry studies.

maximum (XAsymMax) are plotted vs. primary energy for data collected by the Pierre Auger Observatory. Predictions for SIBYLL2.1 and QGSJETII03 hadronic models are included.

XAsymMax, is a robust parameter, only slightly dependent on the number of muons at ground. Hence, a possible change in the muon number predictions from models [8] is not expected to introduce significant changes in the mass composition analysis.

The corresponding linear fits of both primary types are clearly separated, thus allowing discrimination of heavy and light primaries.

As for the parameter $< \Delta_i >$, a calibration with $< X_{\rm max} >$ can be obtained as shown in Figure 6. In addition, the consistency between MC and data and the universality of these correlations were studied. All the calibration curves are in good agreement within the current statistical uncertainties [9].

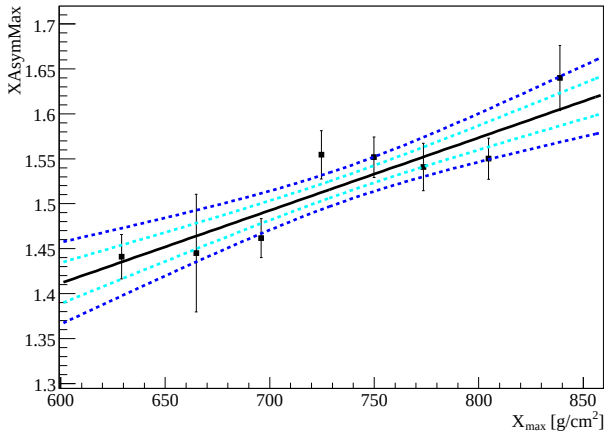


Fig. 6. Calibration curve for data (solid line). Maximum variations (one and two $\sigma$) of the calibration curve when the uncertainties on both fitted parameters are propagated are shown as dashed lines. XAsymMax = a + b $X_{\rm max}$ with a = (0.84 $\pm$ 0.18) and b = (9$\pm$2)10$^{-4}$cm$^2$/g.

## IV. Results and Discussion

With present statistics, the systematic uncertainty in $X_{\rm max}$ obtained due to the parameterisation of the calibration curves are found to be approximately 10 and 16 g cm$^{-2}$ for the risetime and asymmetry methods respectively. The systematic uncertainties are estimated evaluating the half of the variation of $X_{max}$ within the region defined by one $\sigma$ limit curves as shown in Figures 3 and 6.

Figure 7 shows the elongation rate results obtained with both the $< \Delta_i >$ and XAsymMax parameters compared with MC predictions and FD measurements [2]. The results are shown above 3.10$^{18}$ eV, the energy at which the surface detector trigger becomes full efficient for both proton and iron primaries.

Both Figures 7 and 5 (obtained only from SD data) suggest that the mean mass increases with energy.

In addition to the parameters presented above, there are additional approaches to mass composition from SD signals currently under study by the Pierre Auger Collaboration. One of them consists in defining the risetime at 1000 m from the core for each event. The other one use the first portion of the signal, meaning the time to reach from 10% to 30% ($t_{10-30}$) of the total integrated signal in each station. The approach based on the risetime at 1000 m defines a $\Delta(1000)$ but with different benchmarks for different energies. The $t_{10-30}$ is more muon dominated and then may show smaller fluctuations and less sensitivity to asymmetry corrections are expected. Both parameters reach a compatible precision but without the need of any deconvolution of the signal allowing less stringent selection of the surface detector units.

In summary, we have shown the sensitivity of the SD array for determining mass composition with two different approaches. One from pure SD measurements as shown in Figure 5. For the other one the SD array is used to determine $X_{\rm max}$, as shown in Figure 7, from a calibration based on events reconstructed by both SD and FD detectors. Both results are compatible with composition trends indicated from the direct measurements of $X_{\rm max}$ from the FD detectors.

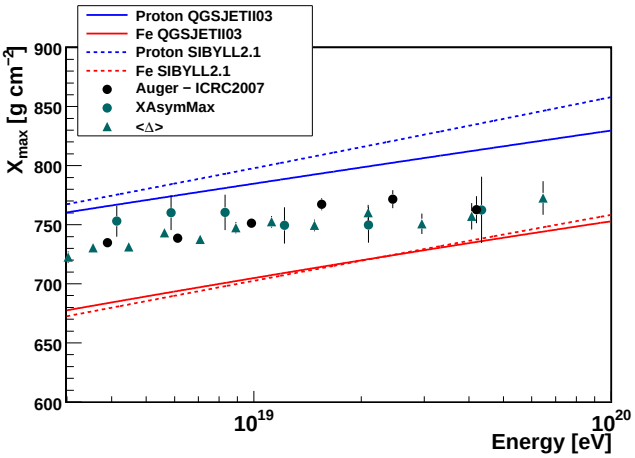


Fig. 7. $X_{\rm max}$ vs. Energy for both parameters. Predictions for a pure iron and pure proton composition according to different models as well as results from direct measurement of $X_{\rm max}$ using the FD [2] are shown for comparison. Uncertainties are only statistical.

## References

[1] J. Abraham *et al.* [Pierre Auger Collaboration], Nucl. Instrum. Meth. A **523**, 50 (2004).
[2] M. Unger *et al.*, Proc. 30th ICRC, Merida, Mexico (2007).
[3] J. Bellido for the Pierre Auger Collaboration, These proceedings.
[4] A.A. Watson. & J.G.Wilson, J. Phys. A **7**, 1199 (1974).
[5] R. Walker & A.A. Watson, J. Phys. G **7**, 1279 (1981).
[6] M. T. Dova, M. E. Mancenido, A. G. Mariazzi, H. Wahlberg, F. Arqueros and D. Garcia-Pinto, Astropart. Phys. **31** 312 (2009).
[7] M. T. Dova for the Pierre Auger Collaboration, Proc. 28th ICRC, Tsukuba, Japan (2003).
[8] A. Castellina for the Pierre Auger Collaboration, These proceedings.
[9] D. Garcia Pinto *et al.*, These proceedings.